Proceedings of the IEEE
International Conference on Information and Automation
Ningbo, China, August 2016

# Cell Out-of-Plane Rotation Control Using a Cell Surgery Robotic System Equipped with Optical Tweezers Manipulators

Mingyang Xie, Shuxun Chen, James K. Mills, Yong Wang, Yunhui Liu, and Dong Sun

***Abstract*—Single cell surgery has been gaining increasing attention due to its extensive applications in physiological and pathological of cell research. Orientation control of biological cell is a basic and vital technique required in cell surgery procedures. By adjusting the orientation of the cell appropriately, the components and sites of interest can be captured by a microscope, such that further analysis, diagnosis, extraction and treatment can be performed. Cell rotation reduces the potential unwanted damage to components of cell during cell surgery. Currently, orientation control of biological cells is typically carried out with manual operations. With ongoing trend towards automated manipulation, a framework that can automate the multi-axis rotation of suspended biological cells is urgently needed. In this paper, we utilize two optical traps, generated by robotically controlled holographic optical tweezers (HOT), as two special manipulators to manipulate the cell for out of image plane rotation. By utilizing the T-matrix approach and experimental calibration, the relationship between the relative vertical height of the optical traps and the rotational angle is characterized. A visual feedback controller is further developed to rotate the cell to the pre-determined orientation accurately. Experiments are performed to demonstrate the effectiveness of the proposed approach.**

This work was supported by grants from the Research Grants Council of Hong Kong Special Administrative Region, China. [Reference No. CityU11210135 and CUHK/CRF/13G].

Mingyang Xie is with the Department of Mechanical and Biomedical Engineering, City University of Hong Kong, Hong Kong, and also with the Department of Automation, University of Science and Technology of China, China (e-mail: xmingyang2-c@cityu.edu.hk).

Shuxun Chen is with the Department of Mechanical and Biomedical Engineering, City University of Hong Kong, Kowloon, Hong Kong (shuxuchen2@cityu.edu.hk).

James K. Mills is with the Department of Mechanical and Industrial Engineering, University of Toronto, Toronto, Ontario, Canada (mills@mie.utoronto.ca).

Yong Wang is with the Department of Automation, University of Science and Technology of China, China (e-mail: yongwang@ustc.edu.cn).

Yunhui Liu is with the Department of Mechanical and Automation Engineering, the Chinese University of Hong Kong, Shatin, N. T., Hong Kong (yhliu@mae.cuhk.edu.hk).

Dong Sun is with the Department of Mechanical and Biomedical Engineering, City University of Hong Kong, Kowloon, Hong Kong (Phone: 852-34428405; Fax: 862-34420172; E-mail: medsun@cityu.edu.hk).

## I. INTRODUCTION

Recently, single cell surgery techniques have gained much attention, due to their extensive applications in physiological and pathological of cell research. Some examples are in vitro fertilization (IVF) [1], preimplantation genetic diagnosis (PGD) [2], intracytoplasmic sperm injection (ICSI) [3]; cloning techniques [4]; introducing exogenous nucleic acids (RNA, DNA) into the cell for the creation of transgenic organisms to investigate the functions of genes and proteins [5]; removal of organelles and/or subcellular components to diagnose and treat the diseases caused by the dysfunction of these components [6]; mechanical characterization of biological cells for identifying the pathological condition of a cell [7]; evaluating drug efficacies [8], to name a few. Orientation control of biological cells is a basic and vital step required during the cell surgery procedures. For example, in the process of IVF, oocytes should be in a proper orientation so that sperm can access to it easily. In the procedure of PGD, ICSI, and organelle extraction, the biological cell must first be oriented properly so that polar body, organelle or desired components can be visualized with a microscope. Then micromanipulation tools are placed at the correctly oriented site to access the target and avoid causing damage to the cell components. When delivering materials into a cell, such as nucleic acid, utilizing a micropipette, the cell must also be oriented correctly for successful execution of this procedure, while avoiding damage to other components. Therefore, controlled cell orientation is a necessary and important technique required in single cell surgery.

Currently, a significant effort has been taken towards achievement of cell orientation control. For example, by utilizing the gradient of an electric field, dielectrophoresis (DEP) has been adopted in many research groups to rotate biological cells [9, 10]; however, the manual open loop operation and the limited rotational degrees of freedom limit the application of this approach. Magnetic fields have been used to reorient biological cells [11], by which the cell was only aligned with the magnetic lines. Fluidic flow has also been applied for the achievement of cell rotation [12], but without active control of cell orientation when performing out of plane rotation. Due to the advantages of precise, flexible, non-invasive manipulation of micro/nano particles, optical tweezers have been widely used to reorient biological cells [13-15]. However, the vast majority of these reported approaches are performed in a manual manner and/or are limited by the number of DOF of rotation possible. In our previous works [16, 17], a robotically controlled holographic

978-1-5090-4102-2/16/$31.00 ©2016 IEEE

optical tweezers system were developed to achieve automated cell in-plane rotation. Up to now, few works have examined the problem of cell rotation out of the image plane. With ongoing development towards automation of cell manipulation applications [18-21] and the demand to increase biological cell processing accuracy and complexity, an automated framework that can achieve multiple degrees of freedom of cell rotation is needed urgently.

In this paper, we propose to utilize two optical traps as two special manipulators to rotate a suspended cell out-of-plane automatically. Here the plane refers to the horizontal image plane, as seen by the microscope used to image the process. One of the optical traps is placed at the center of the cell to stabilize the cell position, the other optical trap placed at the edge of the cell to rotate the cell out-of-plane, by varying the vertical height. Based on T-matrix approach for modelling the forces and torques generated by optical tweezers [27] and experimental calibration, the relationship between the relative vertical height of the two optical traps and out of image plane rotational angle is calibrated linearly. Based on the dynamic model of the rotated cell and the calibrated results, a visual feedback controller is developed to perform cell out-of-plane rotation to achieve a desired orientation. Experiments are performed to demonstrate the performance of the proposed approach. The work reported here is the first application of laser tweezers to carry out controlled out-of-plane rotation of a single cell. This paper also reports for the first time, the use of torsional stiffness to characterize the mechanical properties of optical tweezers.

The remainder of this paper is organized as follows. The robot-tweezer system and the dynamic model of the rotated cell are introduced in section II. Section III presents the development of a visual feedback controller for cell out of plane rotation. Experimental results are reported in section IV, which is followed by the conclusions of this work given in Section V.

## II. ROBOT-TWEEZER SYSTEM AND DYNAMIC ANALYSIS

### A. Robotically Controlled Optical Tweezers System

The optical forces and torques that allow control of the position and orientation of biological cells result from the transfer of linear and angular momentum from photons to the cell when a focused beam of light passes through the biological cell [22]. Optical tweezers is used as an optical trapping device that can trap and manipulate particle ranging from tens of nanometers to tens of micrometers in a noninvasive manner [23-25]. Utilizing holographic technology, multiple optical traps can be produced to manipulate a group of biological cells simultaneously. A robotically controlled holographic optical tweezers (HOT) was set up in City University of Hong Kong [26], as shown in Fig. 1. The system includes three modules, namely, a sensory module, a control module, and an executive module. The sensory module consists of an inverted microscope and a CCD camera. The control module contains a motion controller for the motorized stage, a phase modulator for the HOT device, and a host computer. The executive module consists of a *XYZ* motorized stage and a HOT device, which can vary the relative position between the optical trap and biological cell.

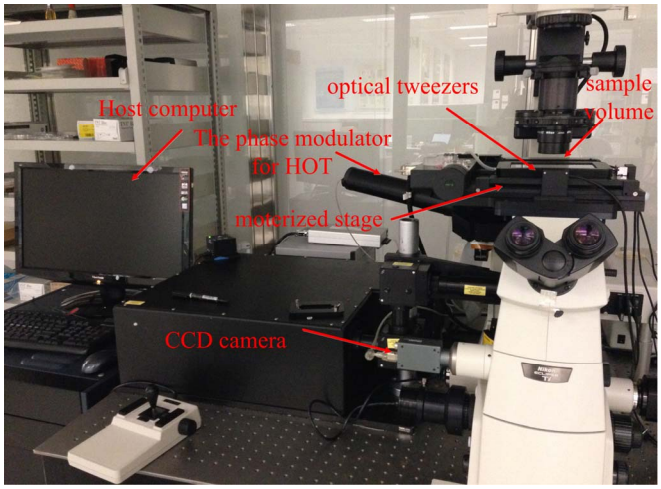


Fig. 1. Robot manipulation system equipped with holographic optical tweezers.

### B. Dynamic Analysis

The applied optical force and torque on a biological cell, under the action of a single optical trap, is illustrated in Fig. 2 [16]. Two coordinate frames are defined to describe the dynamic model of the manipulated cell. The first coordinate frame is the inertial frame *O-XYZ* fixed in the space. The second coordinate frame is body frame *o-xyz* attached to the center of mass *o* (*CM*) of the cell. The applied force and torque from the optical trap with respect to the body frame are denoted as *F* and *T*, respectively. The position of the optical trap applied within the cell with respect to *o* is given by *u*, which can also be described as $(r,\theta,\varphi)$ in spherical coordinates, as illustrated in Fig. 2. The angular velocity of the cell rotation with respect the inertial frame is given by $\omega(t)$.

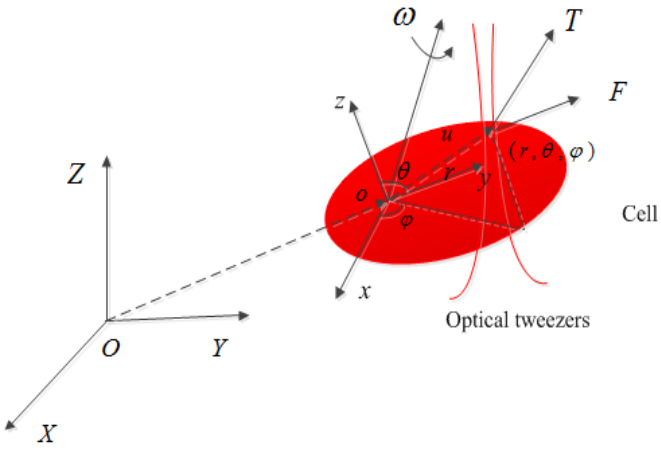


Fig. 2. Schematic of the applied force and torque on the cell due to the action of the optical trap. *O-XYZ* is the inertial frame, *o-xyz* is the body frame. $(r,\theta,\varphi)$ is the spherical coordinates of the applied optical trap with respect to the body frame [16].

Referring to the authors' previous results [16], the relationship between the applied torque and optical trapping spherical coordinates within the cell can be characterized by utilizing a T-matrix approach for computational modelling of optical tweezers [27]. By employing two optical traps applied at symmetric positions about the cell *CM* in the *XY* plane, where the two optical traps hold the edges of the cell, the biological

cell is rotated about the $Z$ axis when moving the two traps in a circular trajectory, maintaining contact with the cell edge [16, 28].

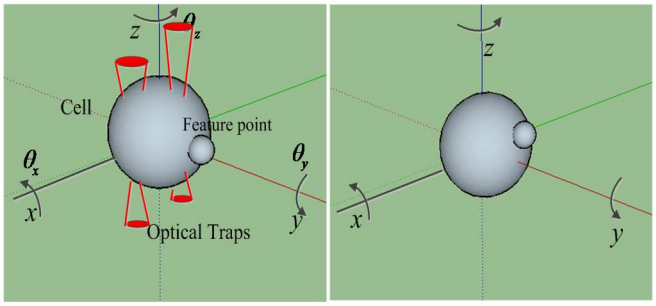


(a)

Top View

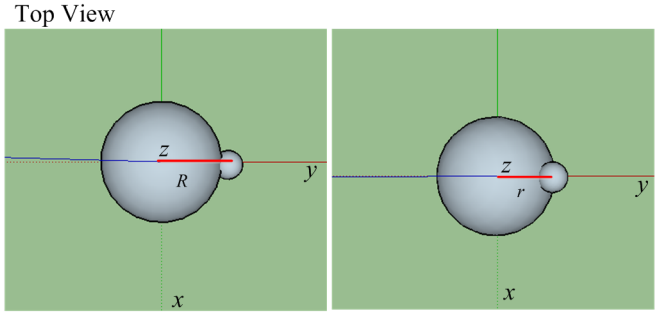

(b)

Front View

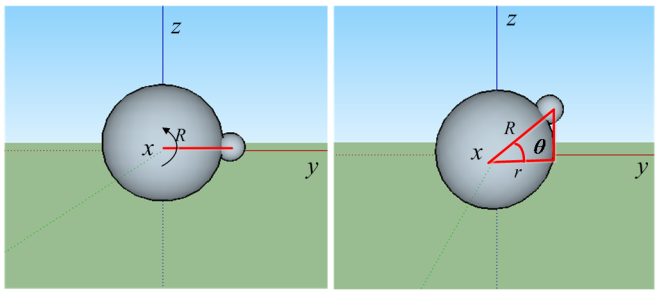

(c)

Fig. 3. (a) Schematic diagram of cell out of plane rotation under the action of two optical traps. (b) The top view of cell rotation, and the cell arrives at a new orientation after the cell rotating an angle $\theta$. (c) The Front view of cell rotation.

In this paper, we use two optical traps, initially located on the cell $XY$ plane to perform cell out of image plane rotation. The cell can be rotated out of the image plane by adjusting the relative vertical height of the two optical traps in the $Z$ axis direction, as shown in Fig. 3(a). The detailed force and torque analysis of the rotated cell is similar to that of cell rotation along $Z$ axis [16] and hence is omitted here. The applied force and the component of the torque in the $Z$ axis from the two optical traps is cancelled, and only the components of torque in the $X$ and $Y$ axis is exerted on the cell. Therefore, the cell can be rotated out of the image plane about the $X$ axis out of the $XY$ plane, and rotational axis is perpendicular to the line that the plane of the two optical traps intersects with the $XY$ plane. Fig. 3 shows a schematic of cell rotation about the $X$ axis, out of the $XY$ plane with two optical traps applied, with the two traps symmetrically located with the focal point in the $XY$ plane. Such an out-of-plane rotation using two optical traps will not remarkably stretch the cell, in a similar way to cell in-plane rotation utilizing two optical traps moving along the cell surface [17]. Hence, the rotation model, as illustrated in Fig. 3, is effective.

Similar to the relationship between the optical trapping force and the offset between the cell and the optical tweezers [29], the relationship between the applied torque, denoted as $T$, and the relative vertical height of the two traps is described as:

$$T = K\triangle z \tag{1}$$

where $K$ is the torsional stiffness of the optical traps about the $X$ axis with rotation out of the $XY$ plane, $\triangle z$ is the relative height of the two optical traps and regarded as the control input during the cell out of plane rotational control.

Note that the linear relationship in (1) can be both shown by computational modelling of optical tweezers and experimental calibration, and is given in the second part of section III.

Similar to the dynamic model of the cell motion and in-plane cell rotation about the $Z$ axis, the dynamic equation of cell rotation about the $X$ axis, out of the $XY$ plane, is formulated as follows:

$$I\ddot{\theta} = T\text{-}d_r\dot{\theta} = K\triangle z\text{-}d_r\dot{\theta} \tag{2}$$

where $I$ is the mass moment of inertia at its $CM$ with respect to the body frame, $\theta$ denotes the angle that the trapped cell rotates about the $X$ axis out of the $XY$ plane, $d_r$ is the rotational viscous drag coefficient.

**Remark 1.** The rotational axis of the cell out of plane rotation is perpendicular to the line that the plane of the two optical traps intersects with the $XY$ plane.

## III. VISUAL FEEDBACK CONTROLLER DESIGN

To develop a feedback controller for cell out of plane rotational control, the rotation angle and angular velocity must be acquired by visual extraction algorithms. In this section, we first present the visual algorithm to calculate the rotational angle about the $X$ axis with rotation out of the $XY$ plane, then calibrate torsional stiffness of the optical traps, and finally develop a visual feedback controller.

### *A. Visual Extraction Algorithm*

In this work, we perform automated cell out-of-plane rotation, as shown in Fig. 3. The vision algorithm approach for the calculation of $\theta$ is shown schematically in Fig. 3(b), (c). A cell of interest with a feature point is chosen for the experiment. The subcellular components and/or organelles can also be identified as feature points. The figures in the left-hand side of Fig. 3 (a)-(c) show the initial orientations of the rotated cell, where the center of the cell and the unfocused feature point can be extracted by using the image processing algorithm developed in OpenCV [30, 31]. A robust algorithm was developed to extract the center of the unfocused feature point [32]. The distance between the two centers is hence calculated as $R$. Once the cell is rotated about the $X$ axis in the image plane ($XY$ plane) to a new orientation, the distance between the cell and the feature point can be calculated as $r$, as shown in Fig. 3(b), (c). The following relationship is utilized to estimate the rotational angle $\theta$:

$$\theta = \arccos\frac{r}{R} \tag{3}$$

Note that the cell rotation in a counterclockwise direction is regarded as a positive rotation.

### B. Calibration of the torsional stiffness

Utilizing the aforementioned rotational angle extraction algorithm, the relationship between the relative vertical height of the applied two optical traps and the rotational angle $\theta$ is calibrated with different laser powers that ranged from 0.5 to 2 mW, which represents the torsional stiffness of the optical tweezers. Fig. 4 illustrates the results acquired by the computational modelling method, the experimental data, and the curve fitted to the experimental data, with the laser power set as 1.5 mW. It is shown that the rotational angle $\theta$ increases as the relative vertical height $\triangle z$ of the two optical traps increases within the range $[-\pi/2, \pi/2]$. With the measured experimental data, the torsional stiffness was determined by the slope of the curve fitted by linear least square method. A linear feedback controller was developed by using linear curve fitting method, and the fitting error between the experimental data and theoretical value was small. The fitting slope was 0.1 $um / rad$, as marked in Fig. 4. Based on the computational and experimental results, the relationship between the relative vertical height $\triangle z$ and the rotational angle $\theta$ can be linearized within the range $\theta \in [-\pi/3, \pi/3]$. Therefore, the equation (1) holds under the assumption that $\theta \in [-\pi/3, \pi/3]$. The numerical results were somewhat different from the experimental data due to the refractive index variation when the biological cell was coated to create a feature point.

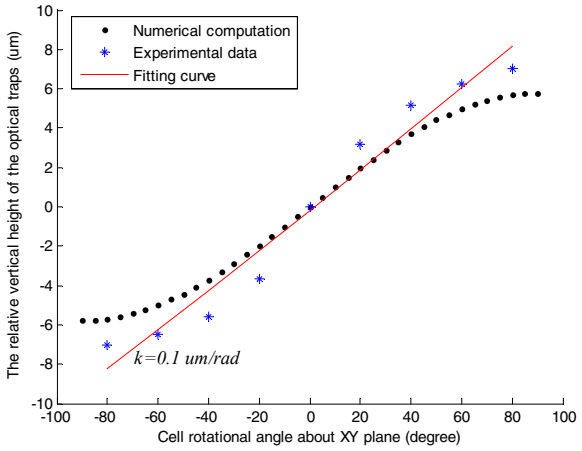


Fig. 4. The relationship between the cell rotational angle about the *X* axis out of the *XY* plane and the relative vertical height of the two applied optical traps. The parameters of the numerical results were set as: laser power P=1.5 mW, the relative refractive index between the suspended cell and the solution is 1.16, and the radius of the cell is 3 $\mu m$.

### C. Controller Design and Stability Analysis

We first formulate the control problem of cell rotational control about the *X* axis out of the *XY* plane as follows:

We first consider a cell of interest with a feature point, and then develop a control input $\triangle z$ for cell out of image plane rotation about the *X* axis out of the *XY* plane to a desired orientation $\theta_d$ in a clockwise or counterclockwise direction.

Based on the dynamic model (2), a visual feedback controller for cell out of plane rotation is developed as follows:

$$\triangle z = k_1 \theta_e + k_2 \dot{\theta}_e \tag{4}$$

where $\theta_e = \theta_d - \theta$ is the angle error, $k_1$ and $k_2$ are positive control gains.

*Theorem 1*. The proposed controller (4) converges the angular error to zero asymptotically, that is $\theta_e \to 0$ as $t \to \infty$.

*Proof*: Substituting (4) into (2), and considering the fact that $\dot{\theta}_d = \ddot{\theta}_d = 0$, the following closed-loop dynamic equation yields:

$$I\ddot{\theta}_e + (k_2 K + d_r)\dot{\theta}_e + k_1 K \theta_e = 0 \tag{5}$$

Equation (5) indicates that $\theta_e \to 0$ as $t \to \infty$, because all the roots of (5) have negative real parts since all parameters and control gains are positive. Hence, the proof of *Theorem 1* is completed.

## IV. EXPERIMENTS

Experiments were carried out to illustrate the performance of the proposed method to rotate the biological cell out of the image plane. The proposed visual feedback controller (4) was used to rotate a yeast cell with the robot-aided holographic optical tweezers. The yeast cell with a bud, denoted as the feature point, was selected for cell rotational control. The dry yeast powder were dissolved in pure water solution, then assembled with microscopic slides and cover slips, and finally put onto the sample volume. The images of the yeast cells were captured using a CCD camera ( $640 \times 480$ pixels) under a converted $60\times$ microscope, and the conversion coefficient from the image pixel to metric units was calibrated as 0.12 $\mu m / pixel$ previously [20]. The angular position of the cell was acquired by using the aforementioned visual extraction algorithm. The control gains were set as $k_1 = 10$, and $k_2 = 10$. The laser power for each optical trap was set as 1.5 $mW$. In the experiments conducted, the two optical traps applied were symmetrical in the *XY* plane along the *Y* axis, hence the cell was just rotated out of plane about the *X* axis.

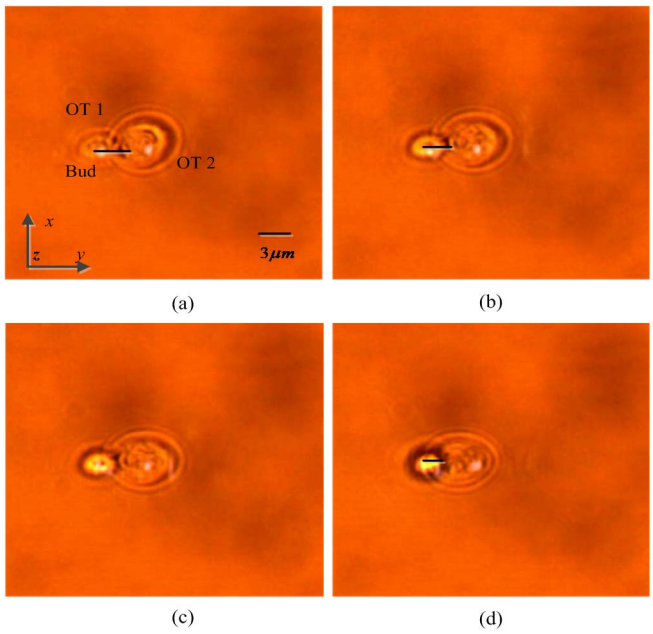

Fig. 5. Snapshots of cell out of plane rotation about the *X* axis by utilizing two optical traps. (a) The initial orientation of the yeast cell trapped by two optical tweezers $\theta = 0^{\circ}$. (b) Orientation of the cell after rotating an angle $\theta = -36^{\circ}$. (c) $\theta = -41^{\circ}$. (d) The final orientation of the cell after rotating the desired angle $\theta = -60^{\circ}$.

Fig. 5 shows the orientations of the yeast cell with radius 3 $\mu m$ at different times under the action of controller (4). Note that the yeast cell with its bud was placed on the image plane of the CCD camera through manual manipulation with the optical tweezers prior to the start of rotational experiments. As shown in Fig. 5(a), two optical traps, denoted as OT 1 and OT 2, respectively, were applied onto the yeast cell. By altering the vertical coordinate of OT 1, while OT 2 was fixed to stabilize the cell and prevent it from translating during the procedure of cell rotation, the cell was rotated about the *X* axis in a clockwise direction under the action of the controller (4), as shown in Fig. 5(b)-(c), gradually. Finally, the cell was rotated to its desired orientation successfully, as illustrated in Fig. 5(d), the bud is shown partially rotated out of image plane. Some additional cells which were not part of the experiment may move into the workspace due to Brownian movement during the process of cell rotational control. Fig. 6 demonstrates the angular error response during the process of cell rotation. It is seen that the angular error converges to zero approximately exponentially.

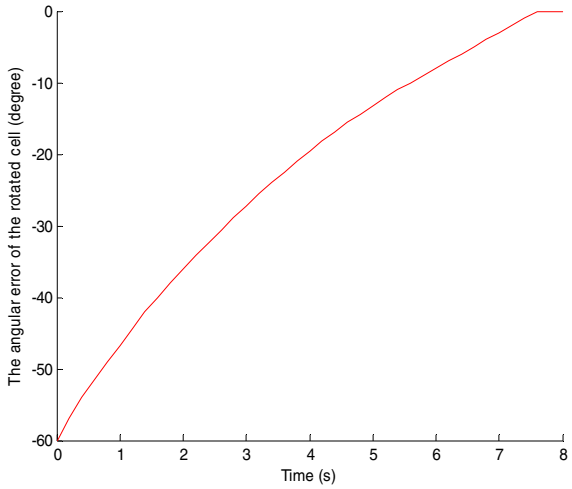


Fig. 6.The time response of the angular error during the cell out of plane rotation about the *X* axis in a clockwise direction.

Note that since the mass moment of inertia of the cell at its *CM* is negligible in a low Reynolds number environment, the dynamic model of cell rotation dynamics, describe in eq. (2), is regarded as first order. Therefore, the angular error exhibits an approximately exponential response.

In the second experiment, we perform cell out-of-plane rotation about the *X* axis in a counterclockwise direction. Fig. 7 and Fig. 8 shows the snapshots of this cell rotation, and the rotational angular error, respectively. As shown in Fig. 7(a), the initial orientation of the cell about the *X* axis is defined as when the bud is rotated partially out of the image plane. Gradually, the cell is rotated so that the bud lies in the image plane due to cell rotation under the action of controller (4), as shown in Fig. 7(b)-(d). The angular error also finally converges to zero under the action of controller (4).

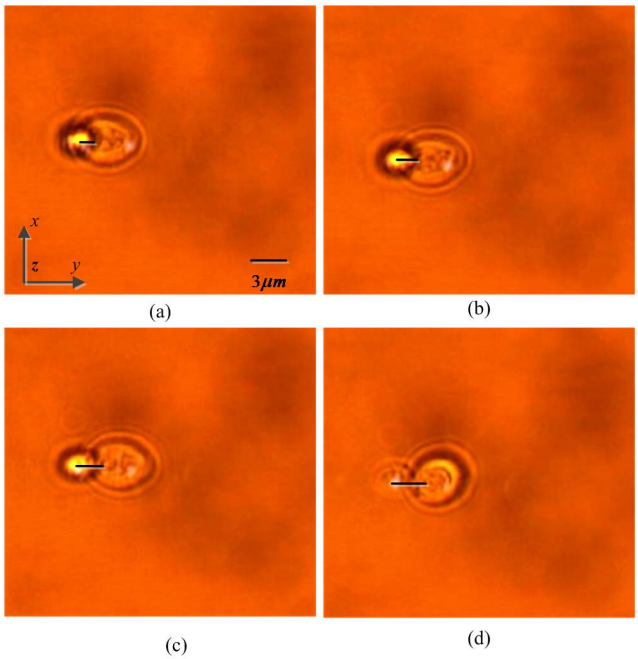


Fig. 7. The snapshots of cell out of image plane rotation in a counterclockwise direction under the action of controller (4). (a) The initial orientation of the cell with $\theta = -60^{\circ}$. (b) The new orientation of the cell $\theta = -48^{\circ}$. (c) $\theta = -36^{\circ}$. (d) The final orientation of the cell $\theta = 0^{\circ}$.

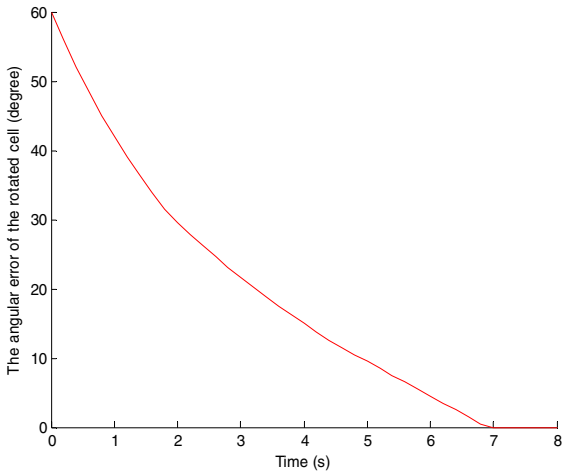


Fig. 8.The time response of the angular error during the procedure of cell out of plane rotation in a counterclockwise direction.

## V. CONCLUSION

In this paper, automated cell out of image plane rotation, manipulated by two optical tweezers manipulators under closed loop control, was presented. Based on the dynamic model of the rotating cell and the visual extraction algorithm, a feedback controller was designed to reorient the cell to the desired orientation. This work fills in the knowledge gap of automated cell out-of-image plane rotation with robot-aided optical tweezers. Torsional stiffness was introduced for the first time to characterize the mechanical property of the action of the optical tweezers. A visual feedback controller was developed to carry

out cell rotation. Experiments were performed to demonstrate the effectiveness of the proposed control strategy. Success of out-of-plane orientation control of biological cell will enable single cells to be oriented properly, hence solving a technical challenging problem faced by cell surgery robotics. Future work will include successful extraction of the cell nucleus and in vitro fertilization by adjusting the orientation of the cell.

## REFERENCES


[1] T. Ebner, M. Moser, O. Shebl, R. Mayer, and G. Tews, "Assisting in vitro fertilization by manipulating cumulus-oocyte-complexes either mechanically or enzymatically does not prevent IVF failure," *J. Turk. Ger. Gynecol Assoc.*, vol. 12, no.3, pp. 135-139, 2011.

[2] L. Gianaroli, "Preimplantation genetic diagnosis: Polar body and embryo biopsy," *Hum. Reprod.*, vol. 15, no. 4, pp. 69–75, 2000.

[3] N. Yoshida and A. C. F. Perry, "Piezo-actuated mouse intracytoplasmic sperm injection (ICSI)," *Nat. Protoc.*, vol. 2, no. 2, pp. 296–304, 2007.

[4] T. Wakayama, A. C. Perry, M. Zuccotti, K. R. Johnson, and R. Yanaqimachi, "Full-term development of mice from enucleated oocytes injected with cumulus cell nuclei," *Nature* 394, pp. 369-374, 1998.

[5] E. Lam, P. N. Benfey, P. M. Gilmartin, R. X. Fang, and N. H. Chua, "Site-specific mutations alter in vitro factor binding and change promoter expression pattern in transgenic plants," *Proc. Nat. Acad. Sci.*, vol. 86, no. 20, pp. 7890–7894, 1989.

[6] J. Ando, G. Bautista, N. Smith, K. Fujita, and V. R. Daria, "Optical trapping and surgery of living yeast cells using a single laser," *Rev. Sci. Ins.,* vol. 79, 2008.

[7] Y. Tan, D. Sun, J. Wang, and W. Huang, "Mechanical characterization of human red blood cells under different osmotic conditions by robotic manipulation with optical tweezers," *IEEE Trans. Biomed. Eng.*, vol. 57, no. 7, pp. 1816–1825, Jul. 2010.

[8] A. Vogel, J. Noack, G. Huttman, G. Paltauf, "Mechanisms of femtosecond laser nanosurgery of cells and tissues," *Appl. Phys. B*, vol. 81, pp. 1015–1047, 2005.

[9] R. Kunikata, Y. Takahashi, M. Koide, T. Itayama, T. Yasukawa, H. Shiku, and T. Matsue, "Three dimensional microelectrode array device integrating multi-channel microfluidics to realize manipulation and characterization of enzyme-immobilized polystyrene beads," *Sens. Actuators B, Chem.*, vol. 141, no. 1, pp. 256–262, 2009.

[10] C. Jiang, and J. K. Mills, "Planar cell orientation control system using a rotating electric field," *IEEE/ASME Trans. Mech.*, vol. 20, no. 5, pp. 2350-2358, 2015.

[11] M. Ogiue-Ikeda and S. Ueno, "Magnetic cell orientation depending on cell type and cell density," *IEEE Trans. Magn.*, vol. 40, no. 4, pp. 3024–3026, Jul. 2004.

[12] C. Leung, Z. Lu, X. Zhang, and Y. Sun, "Three-dimensional rotation of mouse embryos," *IEEE Trans. Biomed. Eng.*, vol. 59, no. 4, pp. 1049–1056, Apr. 2012.

[13] E. Higurashi, R. Sawada, and T. Ito, "Optically induced rotation of a trapped micro-object about an axis perpendicular to the laser beam axis," *Applied Physics Letters*, vol. 72, no. 23, pp. 2951, 1998.

[14] S. Bayoudh, T. A. Nieminen, N. R. Heckenberg, and H. Rubinsztein-Dunlop, "Orientation of biological cells using plane-polarized gaussian beam optical tweezers," *J. Mod. Opt.*, vol. 50, no. 10, pp. 1581–1590, 2003.

[15] S. Mohanty, "Optically-actuated translational and rotational motion at the microscale for microfluidic manipulation and characterization," *Lab Chip*, vol. 12, no. 19, pp. 3624-3636, 2012.

[16] M. Xie, J. K. Mills, X. Li, Y. Wang, and D. Sun, "Modelling and control of optical manipulation for cell rotation," *IEEE Int. Conf. Robot. Autom.*, Seatle, USA, 2015, pp. 956-961.

[17] M. Xie, J. K. Mills, Y. Wang, M. Mahmoodi, and D. Sun, "Automated translational and rotational control of biological cells with a robot-aided optical tweezers manipulation system," *IEEE Trans. Autom. Sci. Eng.*, on line.

[18] Y. Sun, and B. J. Nelson, "Biological cell injection using an autonomous microrobotic system," *Int. J. Robotics Research*, vol. 21, pp. 861-868, 2002.

[19] M. Xie, Y. Wang, G. Feng, and D. Sun, "Automated pairing manipulation of biological cells with a robot-tweezers manipulation system," *IEEE ASME Trans. Mech.*, vol. 20, no. 5, pp. 2242-2251, 2015.

[20] H. Chen and D. Sun, "Moving groups of microparticles into array with a robot–tweezer manipulation system," *IEEE Trans. Robotics*, vol. 28, no. 5, pp.1069-1080, 2012.

[21] S. Chowdhury, A. Thakur, P. Svec, C. Wang, W. Losert, and S. K. Gupta, "Automated manipulation of biological cells using gripper formations controlled by optical tweezers," *IEEE Trans. Auto. Sci. Eng.*, vol. 11, no. 2, pp. 338–347, 2014.

[22] A. Ashkin, J. M. Dziedzic, and T. Yamane, "Optical trapping and manipulation of single cells using infrared laser beams," *Nature* 330, pp. 769-771, 1987.

[23] K. C. Neuman, and S. M. Block, "Optical trapping," *Rev. Sci. Instrum.*, vol. 75, no. 9, pp. 2787-2809, 2004.

[24] S. C. Chapin, V. Germain, and Eric. R. Dufresne, "Automated trapping, assembly, and sorting with holographic optical tweezers," *Opt. Express*, vol. 14, no. 26, pp. 13095-13100, 2006.

[25] A. G. Banerjee, S. Chowdhury, and S. K. Gupta, "Optical tweezers: Autonomous robots for the manipulation of biological cells," *IEEE Robotics and Autoamtion Magainze*, vol. 21, no. 3, pp. 81-88, 2014.

[26] Y. Wu, D. Sun, and W. Huang, "Mechanical force characterization in manipulating live cells with optical tweezer," *J. Biomech.*, vol. 44, pp. 741–746, 2011.

[27] T. A. Nieminen, V. L. Y. Loke, A. B. Stilgoe, N. R. Heckenberg, and H. Rubinsztein-Dunlop, "T-matrix method for modelling optical tweezers," *J. Mod. Opt.*, vol. 58, pp. 528-544, 2011.

[28] F. Horner, M. Woerdemann, S. Muller, B. Maier, and C. Denz, "Full 3D translational and rotational optical control of multiple rod-shaped bacteria," *J. Biophoton*, vol. 3, pp. 468-475, 2010.

[29] Y. Wu, D. Sun, W. Huang, and N. Xi, "Dynamics analysis andmotion planning for automated cell transportationwith optical tweezers," *IEEE/ASME Trans. Mechatronics*, vol. 17, no. 4, pp. 706-713, 2012.

[30] K. R. Castleman, *Digital Image Processing*. Englewood Cliffs, NJ, USA: Prentice-Hall, 1996.

[31] G. Bradski and A. Kaebler, *Learning OpenCV*. Sebastopol, CA, USA: O'Reilly Media, 2008.

[32] B. Y. Yu, C. Elbuken, C. L. Ren, and J. P. Huissoon, "Image processing and classification algorithm for yeast cell morphology in a microfluidic chip," *J. Biomed. Opt.*, vol. 16, no. 6, p. 066008, 2011.